EDWA-LR-72-0041

EFFECT OF PRESSURE ON THE FERROMAGNETIC TRANSITION OF MnAs$_x$Sb$_{1-x}$ SOLID SOLUTIONS[*]

L. R. Edwards and L. C. Bartel

Sandia Laboratories, Albuquerque, New Mexico 87115

ABSTRACT

The ferromagnetic transition temperature of MnAs$_x$Sb$_{1-x}$ solid solutions for $0 \le x \le 1$ have been measured as a function of pressure up to 4.5 kbar. Previous work has shown that for the solid solutions in the concentration range $0.9 \lesssim x \le 1$ the magnetic transition is first-order and is accompanied by a hexagonal to ortho-rhombic structure transformation, while for $0 \le x \lesssim 0.9$ the magnetic transition is second-order with no structural change. We have found that the initial pressure derivative of the transition temperature, $\partial T_c/\partial P$, changes discontinuously in the narrow concentration range $0.87 \lesssim x \le 0.90$, further demarcating the first and second-order regions. We show that an itinerant electron ferromagnet model can be applied to the solid solutions which exhibit second-order behavior. From the experimental values of $\partial T_c/\partial P$ a minimum value of the Stoner enhancement factor, $(\overline{I} - 1)^{-1}$, is estimated for the second-order solid solutions. We also find that substituting Sb for As in the first-order region increases the critical pressure, P_c, which stabilizes the orthorhombic phase to lowest temperature. This further supports Goodenough's observation of a critical molar volume range in which the first-order transformation occurs.

I. INTRODUCTION

The isomorphic metallic compounds MnAs and MnSb have different magnetic properties which are believed to be due to differences in the Mn-Mn separation distance. For increasing temperature, MnAs exhibits a first-order ferromagnetic (FM) to paramagnetic (PM) transition at 313°K which is accompanied by a change in crystal symmetry from the hexagonal NiAs structure $(B 8_1)$ to the orthorhombic MnP structure (B 31). (Hereinafter we use FM to denote ferromagnetic, ferromagnet, or ferromagnetism, and similarly for PM.) On further heating, a second-order transition involving a change from a low-spin PM to a high-spin PM phase and a change in crystal symmetry from the orthorhombic (B 31) to hexagonal structure $(B 8_1)$[1] is observed at 398°K. On the other hand, MnSb has a second-order FM to PM transition at 572°K with the crystal structure remaining hexagonal $(B 8_1)$ through the transition.[2] A complete series of solid solutions is formed by MnAs and MnSb in which the hexagonal lattice parameters decrease monotonically from MnSb to MnAs.[3]

The various magnetic transition temperatures and crystal structures of the solid solutions $MnAs_xSb_{1-x}$ as reported by Sirota and Vasilev[4] and Goodenough et al.[5] are summarized in Fig. 1. Here, for increasing temperature, T_c denotes the FM to PM transition temperature, T' denotes the PM to PM transition temperature at which the effective moment decreases, and T_t is a PM to PM transition temperature at which the effective moment increases and the crystal structure changes from orthorhombic to hexagonal. For the solid solutions in the concentration range $0.9 \leq x \leq 1.0$ the transition from the FM hexagonal phase to the PM orthorhombic phase is first-order. All other transitions are second-order.

From Fig. 1 we see that over the concentration range $0 \leq x \leq 0.80$ the FM to PM transition temperature, T_c, decreases with increasing As concentration. In addition, the effect of substituting As for Sb is to decrease the lattice

parameters[3] (decrease the Mn-Mn separation distance); thus one might expect T_c to be quite sensitive to pressure and to decrease with the application of pressure. As we shall report on in Sec. III, we have observed a decrease in T_c with increasing pressure for solid solutions in this concentration range.

Goodenough and co-workers have proposed a band model to explain some of the magnetic properties of MnAs.[1,5,6] The essential features of their model are a filled s-p bonding (valence) band and an empty s-p antibonding (conduction) band where the Fermi energy lies between the bonding and antibonding bands, and the Mn 3-d states lie near the Fermi energy. In the hexagonal FM phase the crystalline field splits the Mn 3-d states into three distinct energy levels labeled t_o, $t_\pm$, and e_g.[6] The t_o orbital is directed toward the near neighbor (nn) Mn along the c-axis, the two $t_\pm$ orbitals are directed toward nn Mn in the basal plane, and the two e_g orbitals are directed toward nn As. It is also argued that there is a critical Mn-Mn separation, $R_c \sim 3.1$-3.7Å, such that an itinerant description is used if the Mn-Mn separation is less than R_c and a localized description is used if the Mn-Mn separation is greater than R_c.[1,7] Since the Mn-Mn separation is less than R_c along the c-axis, the t_o and e_g levels broaden into narrow itinerant bands.[8] However, in the basal plane the $t_\pm$ levels are transitional since the Mn-Mn separation can be greater or less than R_c depending upon the crystallographic phase. Finally in their model, it is postulated that there is an intra-atomic exchange splitting between the up and down spin bands.

Over the entire concentration range of the solid solutions, the Mn-Mn separation distance along the c-axis remains less than R_c, and thus the t_o and e_g levels should be narrow itinerant bands. One might then expect that an itinerant electron model may describe the pressure dependence of the FM to PM transition. The weak itinerant electron theory as developed by Wohlfarth[9] and

Edwards and Wohlfarth[10] has been used to study the magnetic behavior of such materials as $ZrZn_2$[9] and the Invar alloys.[11] Recently, Wohlfarth and Bartel[12] have shown how to estimate electron correlation effects from pressure measurements for weak itinerant FM's. In Sec. II we extend the itinerant electron model to include the so-called strong itinerant FM's, and we shall show how pressure measurements may be used to determine a minimum value for the Stoner enhancement factor and consequently estimate the correlation effects. This model describes a second-order phase transition, and it will be used to analyze the experimental data presented in Sec. IV for only those solid solutions in the concentration range $x < 0.9$ where these materials exhibit a second-order behavior. In Sec. IV we shall also comment on how inclusion of electron-lattice and exchange-striction effects may be able to explain the first-order nature of the transition for $x > 0.90$.

It has been established in MnAs that above a critical pressure of 4 kbars the orthorhombic phase is stabilized.[1,6] According to Goodenough and Kafalas,[6] the existence of this critical pressure is related to a critical molar volume. Within this critical molar volume there is a high-spin to low-spin transition which they interpret as a "drastic" change in the intra-atomic exchange energy at a maximum critical bandwidth. Then as we substitute Sb for As the lattice expands and the bandwidth decreases so that a higher critical pressure should result for stabilizing the orthorhombic phase. Since the orthorhombic phase exists in the solid solutions only over the concentration range $0.90 \leq x \leq 1$, we have measured the pertinent part of the pressure-temperature magnetic phase diagram of the solid solution $MnAs_{0.90}Sb_{0.10}$. The maximum allowable Sb concentration was chosen to maximize the increase in critical pressure. These results will also be presented in Sec. III and discussed in Sec. IV.

II.   ITINERANT ELECTRON FERROMAGNET MODEL

It is the purpose of this section to present an elementary theory, unifying several existing theories, of a single band, itinerant electron FM. In particular, we shall develop a theory, appropriate for 3-d electrons, for the Curie temperature, T_c, and its pressure derivative, $\partial T_c/\partial P$; and we shall show how estimates of the effective exchange, I, times the density of states at Fermi level, $N(\epsilon_F)$, can be made from the measurements of $\partial T_c/\partial P$. The theory presented here follows quite closely the earlier work of Wohlfarth,[9] Edwards and Wohlfarth,[10] Shiga,[13] and Wohlfarth and Bartel,[12] but includes details which have not been discussed in these earlier works.

For our model we assume that the exchange splitting is given by $nI\zeta$ where I is the effective intra-atomic exchange (accounting for the electron correlations) between the itinerant electrons, n is the number of d-electrons per atom, and ζ is the relative magnetization per electron arising from single-particle excitations. In the Stoner theory, the exchange splitting is $2k_B\theta'\zeta$ where $k_B\theta'$ is the molecular field approximation interaction; thus $k_B\theta' = 1/2\ nI$. The single particle excitations are described by the Stoner equations[9,10]

$$1/2\ n(1 \pm \zeta) = \int_0^\infty f(\epsilon,\eta^\pm)\ N(\epsilon)\ d\epsilon \qquad , \qquad (1)$$

where

$$f(\epsilon,\eta) = \left\{ \exp\left[(\epsilon - \eta)/k_B T\right] + 1 \right\}^{-1} \qquad ,$$

and

$$\eta^\pm = \mu \pm 1/2\ nI\zeta \pm \mu_B H \qquad .$$

Here μ is paramagnetic chemical potential, H is the applied magnetic field, and $N(\epsilon)$ is the density of states. In the limit as $T \to T_c$ such that $\zeta \to 0$ and

letting H = O, we can expand the Fermi function exponentials in the expression for ζ, Eq. (1), and obtain the well known result

$$I \int_{0}^{\infty} N(\epsilon) \left| \frac{\partial f}{\partial \epsilon} \right|_{\substack{T=T_c \\ H=O}} d\epsilon = 1 \quad . \tag{2}$$

Within the framework of the model, Eq. (2) can be solved for T_c if $N(\epsilon)$ is known. Even if we don't know $N(\epsilon)$ we can solve Eq. (2) by use of the Sommerfeld expansion. To terms quadratic in T_c we obtain[14]

$$T_c^2 = T_F^2 (\overline{I} - 1) / \overline{I} \quad , \tag{3}$$

where

$$\overline{I} = I N(\epsilon_F) \quad . \tag{4}$$

Here $N(\epsilon_F)$ is the density of states per atom per spin at the paramagnetic Fermi level, and T_F is the effective degeneracy temperature defined by[9,10]

$$T_F^2 = \left\{ \frac{\pi^2}{6} \, k_B^2 \left[\left(\frac{N'(\epsilon_F)}{N(\epsilon_F)} \right)^2 - \frac{N''(\epsilon_F)}{N(\epsilon_F)} \right] \right\}^{-1} \quad , \tag{5}$$

where $N^{(m)}(\epsilon_F)$ is the m-th derivative with respect to energy evaluated at ϵ_F. The expression for T_c^2, Eq. (3), is identical to what one would obtain from the singularity in the exchange enhanced susceptibility where the F-integral of Lang and Ehrenreich[15] is expanded by means of a Sommerfeld expansion. In order for the system to be FM, we have from Eq. (3) the Stoner criterion, $\overline{I} \geq 1$.

The expression for T_c^2, Eq. (3), is general to the extent that we have not specified the origin or nature of I and we have not restricted $N(\epsilon_F)$. To find

the pressure dependence of T_c requires knowledge of the pressure dependencies of T_F, $N(\epsilon_F)$, and I. In the following discussion we shall make some assumptions as to the nature of I and $N(\epsilon_F)$.

Let us assume that the FM behavior can be described by the Hubbard model[16] for a single, nondegenerate, d-band orbital, such as discussed by Evenson et al.,[17] where the bare intra-atomic exchange constant is replaced by an effective intra-atomic exchange which takes into account the individual electron correlations. In general we assume that I is a compositionally averaged constant in the case of the FM behavior of alloys. For the $MnAs_x Sb_{1-x}$ solid solutions considered in this paper, I is the effective exchange appropriate for the Mn atoms. Using double time Green's function techniques and decoupling in first order, the exchange splitting is the assumed $nI\zeta$.[18] We assume that I can be found by means of a perturbation treatment such as used by Lang and Ehrenreich[15] or by Kanamori,[19] and we write I as given approximately by[12,13,15,19]

$$I = I_b \left(1 + \gamma I_b / W\right)^{-1} \qquad , \qquad (6)$$

where I_b is the bare interaction, W is the bandwidth and γ is a constant. In addition we assume that the number of magnetic electrons n remains constant,[20] consequently $N(\epsilon_F)$ can be written as[12,13]

$$N(\epsilon_F) = \beta / W \qquad , \qquad (7)$$

where β is another constant and is related to γ. It is implied that W and thus $N(\epsilon_F)$ scale uniformly (uniform scaling assumption) under volume changes. Finally, we assume the volume dependence of W is given by Heine's[21] results

$$\partial \ln W / \partial \ln V = - 5/3 \qquad . \qquad (8)$$

Using the above results, Eqs. (6)-(8), the volume dependence of $\overline{I}$, Eq. (4), is

$$\frac{\partial \ln \overline{I}}{\partial \ln V} = \left[\frac{5}{3} + \frac{\partial \ln I_b}{\partial \ln V} \right] \frac{I}{I_b} \quad , \tag{9}$$

which is independent of β and γ and where here I_b is assumed volume dependent. For the density of states of the form given by Eq. (7), it can be shown that $T_F \sim W$, and hence from Eq. (8), $\partial \ln T_F / \partial \ln V = -5/3$. Using Eqs. (3), (4), (8) and (9) the volume dependence of T_c becomes

$$\partial \ln T_c / \partial \ln V \equiv \Gamma$$

$$= - \frac{5}{3} + \frac{1}{2} \left[\frac{5}{3} + \partial \ln I_b / \partial \ln V \right] [\overline{I} - 1]^{-1} (I/I_b) \quad , \tag{10}$$

or equivalently using Eq. (3)

$$\Gamma = - \frac{5}{3} + \frac{1}{2} \left[\frac{5}{3} + \partial \ln I_b / \partial \ln V \right] (I/\overline{I} I_b) (T_F^2 / T_c^2) \quad . \tag{11}$$

In terms of pressure, Eq. (11) can be written as

$$\partial T_c / \partial P = \frac{5}{3} \varkappa T_c + \frac{1}{2} \varkappa \left[\frac{5}{3} + \partial \ln I_b / \partial \ln V \right] (I/\overline{I} \, I_b) (T_F^2 / T_c) \quad , \tag{12}$$

where $\varkappa$ is the volume compressibility.

We shall now show how pressure measurements of T_c can be used to determine a maximum value for $\overline{I}$ and a minimum value for T_F. We can rewrite Eq. (10) as

$$\overline{I} - 1 = \frac{1}{2} \left[\frac{5}{3} + \partial \ln I_b / \partial \ln V \right] (I/I_b) \left[\Gamma + \frac{5}{3} \right]^{-1} \quad . \tag{13}$$

The maximum value that I can have is the bare exchange value I_b; thus, the maximum value for the ratio I/I_b is one. Hence, the experimental value of Γ can be used to determine the maximum values of $\bar{I}$. From Eq. (13) we have

$$\bar{I}_{max} = 1 + \frac{1}{2}\left[\frac{5}{3} + \partial \ln I_b/\partial \ln V\right]\left[\Gamma + \frac{5}{3}\right]^{-1} \quad , \tag{14}$$

which for $\partial \ln I_b/\partial \ln V \cong 0$ reduces to

$$\bar{I}_{max} = 1 + \frac{5}{6}\left[\Gamma + \frac{5}{3}\right]^{-1} \quad . \tag{15}$$

Then using values for $\bar{I}$ obtained from Eqs. (14) or (15) we can obtain a minimum value for T_F using Eq. (3).

For weak itinerant FM's $\bar{I} \gtrsim 1.0$ and for weak electron correlation effect $I/I_b \cong 1.0$; thus the second term in Eq. (10) is dominant, and from Eq. (12) we have $\partial T_c/\partial P \sim -1/T_c$. Examples of weak itinerant FM's are the Fe-Ni, Fe-Pt, and Fe-Pd Invar alloys where it has been experimentally observed that $\partial T_c/\partial P \cong -$ constant$/T_c$.[22] For strong itinerant electron FM's $\bar{I} > 1$ and for strong correlation effects $I/I_b < 1$ such that the first term in Eq. (10) is dominant, and from Eq. (12) we have $\partial T_c/\partial P \sim T_c$. An example of a strong itinerant FM is Ni, where it is found that $\partial T_c/\partial P = (5/3)\varkappa T_c \cong 0.68$ K/kbar in good agreement with experimental values of 0.32-0.42°K/kbar.[9] It is noteworthy that in the limit of weak itinerant FM and for large Γ such that $|\Gamma| \gg 5/3$ and neglecting the volume dependence of I_b, the results of this paper reduce to the results given previously by Wohlfarth and Bartel.[12]

III. EXPERIMENTAL RESULTS

For the preparation of the solid solutions, powders of 99.9% pure Mn, As, and Sb were mixed to the desired proportions, pressed into pellets, sealed in an evacuated quartz tube, and heated to 1073°K for 2 days. The chemically reacted product was then crushed, made into pellets, and annealed at 1073°K for 1 day. There were no observed differences in the magnetic transitions or chemical composition if the samples were quenched in air or were slowly furnace cooled. Chemical analysis of these materials indicated they were stoichimetric to within 4 at.% and the ratio of As to Sb was within 1 at.% of the nominal value. Powder x-ray diffraction patterns indicated the presence of MnO in some of the solid solutions. The presence of MnO should not affect the magnetic transition temperatures of these materials.

The self-inductance technique[23,24] was used to determine the FM to PM transition as a function of pressure and temperature. Hydrostatic pressure was applied with a 4.5-kbar helium gas system[25] on the solid solutions which had transition temperatures less than 323°K and with a Harwood 30 kbar liquid pentane apparatus on the solid solutions which had transition temperatures greater than 323°K. A typical reduced self-inductance versus temperature plot as obtained for the $MnAs_{0.9}Sb_{0.1}$ solid solution is shown in Fig. 2. The transition temperature was arbitrarily taken as the half-transition point.

The experimental results are summarized in Figs. 3-5. In Fig. 3 the FM to PM transition temperature, T_c, is plotted as a function of concentration. The double curve in the concentration range $0.9 \leq x \leq 1.0$ is due to the thermal hysteresis associated with the first-order hexagonal FM to orthorhombic PM transition. No hysteresis is observed for the solid solutions in the concentration range $0 \leq x < 0.90$ which is indicative of a second-order FM to PM transition.

Hereinafter we will refer to $0.9 \leq x \leq 1.0$ as the first-order region and to $0 \leq x < 0.9$ as the second-order region.

In Fig. 4, the initial pressure derivative of the FM to PM transition temperature, $\partial T_c / \partial P$, is plotted as a function of concentration. The pressure derivatives were determined to within $\pm 0.15°K/kbar$. For MnSb our measured pressure derivative of $-3.0°K/kbar$ is in good agreement with the value $-3.2°K/kbar$ as reported by Hirone et al.[26] It is observed that $\partial T_c / \partial P$ changes almost precipitously in a very narrow concentration range ($\sim 3\%$) demarcating the first and second-order regions. It should be remarked that the $x = 0.88$ material exhibited no thermal hysteresis at 4.5 kbar -- indicating that the transition remained second-order up to this pressure limit. (According to the Bean-Rodbell model,[27] it is possible that a second-order transition can be forced into a first-order transition under sufficient pressure; we shall comment more on this in Sec. IV.)

In Fig. 5 a portion of the temperature versus pressure magnetic phase diagram for MnAs and $MnAs_{0.9}Sb_{0.1}$ is shown. Our results for MnAs are in good agreement with the result of Menyuk et al.[1] It is observed, as speculated in Sec. I, that the substitution of 10% Sb for As does indeed increase the critical pressure required to stabilize the orthorhombic phase. The increase in critical pressure is approximately 0.75 - 1 kbar.

IV. DISCUSSION

In part A of this section we will discuss the solid solutions which exhibit second-order behavior. The results on these materials will be analyzed in terms of the itinerant FM model as presented in Sec. II. In part B the alloys which exhibit a first-order behavior will be discussed in terms of the model proposed by Goodenough and Kafalas.[6] In addition, some comments will also be made on the Bean-Rodbell model[27] prediction of pressure induced second-order to first-order behavior and on the equivalence of the itinerant electron FM and the Bean-Rodbell models.

A. Second-Order Behavior

In Fig. 6, $\partial T_c/\partial P$ is plotted as a function of T_c for the $MnAs_x Sb_{1-x}$ solid solutions in the concentration range $0 \leq x \leq 0.8$. For comparison, the Fe-Ni, Fe-Pd, and Fe-Pt Invar alloys data of Wayne and Bartel[22] are included. Similar to the Invar alloys, we observe a T_c^{-1} type of behavior as predicted by Eq. (12) when the second term in Eq. (12) dominates.

The volume derivative of T_c is calculated from $\partial T_c/\partial P$ where the compressibility for the solid solutions was obtained by a linear extrapolation between the values of $2.2 \pm 0.5 \times 10^{-3}$ $kbar^{-1}$ for $MnSb$[28] and 4.55×10^{-3} $kbar^{-1}$ for $MnAs$.[1] The values for Γ are given in Table I. We observe that the values of Γ increase with increasing As concentration and that the magnitude of Γ is of the same order of magnitude as the first term in Eq. (10). In previous works on the Invar alloys[11] and $ZrZn_2$[9-12], it was observed that $\Gamma \gg 5/3$ and so the first term of Eq. (10) could be neglected. In the case of the $MnAs_x Sb_{1-x}$ solid solutions, this factor of $5/3$ must be included in any calculation of band parameters.

In Table I we give the results of the calculation of $\bar{I}_{max}$ from Eq. (15) for the solid solutions $0 \leq x \leq 0.80$ where we assume $\partial \ln I_b/\partial \ln V = 0$. The quoted error in the compressibility for MnSb will introduce an uncertainty of ± 0.03 in the values for $\bar{I}_{max}$. We observe that $\bar{I}_{max}$ decreases with increasing As concentration. According to Wohlfarth's[29] classification, these values of $\bar{I}_{max}$ indicate that MnSb is approaching a strong itinerant FM, and the solid solutions are becoming weaker itinerant FM's with increasing As concentration. These values of $\bar{I}_{max}$ for the $MnAs_x Sb_{1-x}$ solid solutions are comparable with the values for the Invar alloys.[30]

From Eq. (3) and using the value of $\bar{I}$ and T_c for MnSb from Table I, we calculate $T_F = 1380°K$. Thus for MnSb we see that $T_c \cong 0.4 \, T_F$ which indicates the Sommerfeld expansion is converging; however, the convergence is slower than one would desire. For the materials with $x > 0$, the convergence is more rapid than for $x = 0$.

Using Eqs. (3)-(7) we can express T_c as a function of the bandwidth W where we assume $T_F \sim W$. Then using the value of $T_c = 572°K$ and the value of $\overline{I}_{max}$ from Table I for MnSb, we can calculate T_c as a function of W. The results of these calculations are shown in Fig. 7. These results are independent of the value of I/I_b,[31] but do not include effects of any volume dependence of I_b. Note the critical bandwidth such that for $W/W_o \geq 1.206$ we do not have FM order, and note the quadratic dependence of T_c on W for $W/W_o \leq 1.206$ Using the available x-ray data[32] to estimate W/W_o and using the experimental values for T_c we show, in Fig. 7, the experimental results of T_c as a function of W/W_o. For $x = 0.25$ we calculate $T_c = 474°K$ and $\overline{I} = 1.110$ in fair agreement with the experimental values. For the solid solutions $x > 0.25$ the agreement is only qualitative. The disagreement is not too surprising because of the large differences in unit cell volumes for the various compositions. For these large volume differences one might expect significant changes in the crystal field splittings, and consequently significant changes in the electronic wave functions. Any volume dependence of I_b would modify the results shown in Fig. 7. Lacking specific heat, susceptibility, and magnetostriction data for these materials, we cannot determine $N(\varepsilon_F)$, I, I_b, and any volume dependence of I_b individually. In addition, as we shall point out below, we expect rather large electron-lattice and exchange-striction interactions for these materials, particularly for the solid solutions $x \geq 0.80$. Electron-lattice and exchange-striction effects have not been included in the calculations displayed in Fig. 7.

Sirota and Vasilev[4] have observed a Curie-Weiss type of behavior in the PM region for MnSb, with a Curie constant, $C_M = 1.3$ emu mole^{-1}Oe^{-1}°K^{-1}. According to the itinerant FM model of Wohlfarth[9] the susceptibility in the temperature

region $T_F \gg T > T_c$ can be written as

$$\chi = 2\chi_o[T^2/T_c^2 - 1]^{-1} \, , \tag{16}$$

where

$$\chi_o \equiv \frac{N N(\epsilon_F)\mu_B^2}{\bar{I} - 1} \tag{17}$$

Here N is the number of atoms per unit volume. For temperatures near T_c, Eq. (16) can be expanded

$$\chi \simeq \frac{\chi_o T_c}{T - T_c} \, , \quad T \gtrsim T_c \, , \tag{18}$$

which is a Curie-Weiss type of behavior where the Curie constant C_M is given by

$$C_M = \chi_o T_c \, . \tag{19}$$

For MnSb χ_o can be calculated from Eq. (19) to give $\chi_o = 0.227 \times 10^{-2}$ emu mole^{-1}Oe^{-1} as compared to $\chi_o = 1.38 \times 10^{-2}$ emu mole^{-1}Oe^{-1} for ZrZn$_2$.[24] This difference in χ_o between MnSb and ZrZn$_2$ is consistent with the values of $\bar{I}$ for these materials. For ZrZn$_2$ [9] $\bar{I} = 1.0042$ and from this work for MnSb $\bar{I}_{max} = 1.206$; thus from Eq. (17) χ_o for MnSb should be smaller. A detailed comparison, however, can only be made if $N(\epsilon_F)$ for MnSb were known. For $x > 0$, χ_o cannot be reliably extracted from the experimental data because the susceptibility has a complicated temperature dependence[4] which is thought to be due to exchange-striction effects.

The localized and the itinerant, or collective, descriptions of magnetic electrons have been investigated by Goodenough.[33] He considered the case of one d-electron per relevant d-orbital which corresponds to a half-filled band or to half-filled localized orbital, and the magnetic order is antiferromagnetic (AFM). In the absence of competing exchange interactions, the Néel temperature,

T_N, for localized electron AFM increases with the transfer integral, b, since the exchange interaction is proportional to b^2; whereas, it has been shown that T_N for a band AFM decreases with increasing bandwidth[33,34] where the bandwidth is proportional to b. Goodenough concludes that the magnetic moment and T_N should vary continuously in going from a localized to a band description. We expect b to increase with increasing pressure; hence, we expect that for the localized electron description T_N should increase with increasing pressure, and for the itinerant description T_N should decrease with increasing pressure.[34] Furthermore, we expect that the general arguments for an AFM apply to the FM case of interest here. The observed decrease in the FM to PM transition temperature in the $MnAs_xSb_{1-x}$ compounds suggests that the itinerant description is the appropriate one. Although these alloys are anisotropic, the isotropic model discussed in this paper describes the pressure effects quite well.

B. First-Order Region

Previous experimental studies[6] on MnAs and $MnAs_xP_{1-x}$ have established that a first-order hexagonal FM to orthorhombic PM transition occurs only if the molar volume at T_c lies within a narrow critical range $V_t - \Delta V < V < V_t$, where $\Delta V/V \cong 0.025$. This narrow molar volume range is related through the thermal expansion to the temperature range $T_t - 125°K < T < T_t$, where T_t is the second-order orthorhombic PM to hexagonal PM transition temperature. This, coupled with the fact that there is a low-spin $\rightleftarrows$ high-spin transition in this temperature interval, led Goodenough and Kafalas[6] to postulate the existence of a maximum critical bandwidth that would support spontaneous FM and the existence of a volume dependent intra-atomic exchange interaction. This model predicts the existence of a critical pressure, P_c, above which the PM orthorhombic phase is stabilized to absolute zero; a $P_c = 4$ kbar has been found for MnAs.[1,6] If P is

substituted for As, then one expects P_c to decrease since the substitution of P decreases the lattice parameters (the molar volume), and thus the bandwidth increases. Furthermore, if sufficient P is substituted for As, $P_c \rightarrow 0$. These effects have been observed.[5,6] However, if Sb is substituted for As, the lattice parameters (molar volume) increase and the bandwidth decreases. Therefore, the substitution of Sb should cause P_c to increase, which is in accord with our experimental results.

Now if more than 10% Sb is substituted for As, then the molar volume will be larger than the critical volume required for a first-order transition, and the resulting solid solutions exhibit second-order transitions. If this model is correct, then at sufficiently high pressure one might expect to induce a first-order phase change in the materials with concentration $x \leq 0.9$. At the time this work was done, the pressures available to us (~4 kbar) were insufficient to check conclusively this prediction on the $x = 0.88$ solid solution. Estimations based on the isotropic Bean-Rodbell model[27] indicate a second-to-first-order transition pressure of approximately 16 kbar for this material. This number must be taken lightly, however, since there have been objections to using the Bean-Rodbell in its isotropic form for MnAs.[1] We are planning to continue the search for a second-to-first order transition pressure at higher pressure in the solid solutions with concentrations $x \leq 0.9$.

The Bean-Rodbell model,[27] which is based on a localized spin picture, has been used to describe qualitatively the first-order nature of the transition in MnAs. A similar situation arises in the itinerant electron model when the exchange and electron-lattice forces are balanced against the elastic forces. The result of this balance is that the bandwidth and exchange interaction become temperature dependent; then, depending on the parameters, the

transition may tend to sharpen and may become first-order as in the Bean-Rodbell model. This type of procedure has been used to explain thermal expansion effects in an itinerant electron AFM[34] where only the electron-lattice interaction was considered. In this case it was demonstrated that the balance set up between the elastic and electron-lattice forces is important in explaining the anomalous behavior of the thermal expansion for temperatures near T_N. However, for the parameters used in the theory, no first-order nature was observed in the phase transition.[34] It is anticipated that inclusion of exchange-striction effects could precipitate a first-order phase transition for the itinerant electron AFM.

Unpublished x-ray data by Goodenough[35] on $MnAs_{0.80}Sb_{0.20}$ show that the unit cell volume is quite temperature dependent for temperatures near T_c where the volume decreases continuously from a value of $70.81(\overset{\circ}{A})^3$ at a temperature of approximately $100°K$ below T_c to a value of approximately $70.19(\overset{\circ}{A})^3$ at T_c. This represents approximately a 0.9% decrease in the volume. For MnAs there is approximately a 1.8% discontinuous volume decrease at T_c for increasing temperature. It is therefore apparent that for $x \gtrsim 0.80$ there are large interactions of the lattice with the exchange energy and/or the electronic energy. The volume changes associated with these interactions depend on the magnetization. Due to the coupling, a discontinuous change in the unit cell volume is reflected in a discontinuous change in the magnetization, and vice versa.

The physical picture we have for the results of the coupling of the magnetization and the lattice is as follows. At low temperatures the magnetization takes on its saturation value, and the magnetic characteristics are determined by the bandwidth W, density of states $N(\varepsilon_F)$ and the exchange

interaction I. As the temperature is increased the lattice expands, and

due to electron-lattice coupling and exchange-striction, W decreases and

I can either increase or decrease depending on the sign of $\partial \ln I / \partial \ln V$.

For the material under consideration here, as W decreases, T_c will increase

and the magnetization for $T \ll T_c$ will increase over the value it would

have had if W and I did not depend on the volume. However, due to the electron-

lattice and exchange-striction effects, the lattice contracts for $T \lesssim T_c$

and thus W increases and T_c decreases. Hence depending upon the amount of

coupling, the rate at which W increases (or the apparent T_c decreases)

determines whether the transition will be second or first-order. For the

first-order transition, in the words of Bean and Rodbell,[27] ". . . this

situation is like that of a man who has run beyond the brink of a cliff;

there is no gentle way down." The critical volume discussed by Goodenough

and Kafalas[6] appears to be intimately related to the electron-lattice and

exchange-striction effects as a detailed theory should show.

Finally, the rather large changes in T_c with pressure for the first-

order region are noteworthy. As shown in Fig. 4 there is a discontinuous

change in $\partial T_c / \partial P$ at the composition which demarcates the boundary between

the first and second-order regions. In addition, there are strong hysteresis

effects in the first-order region. At this time, we can offer no concrete

explanation of the rather large $(\partial T_c / \partial P)$'s for the first-order region except

to say that the large pressure effects appear to be connected to a "critical

volume"[6] and consequently to the electron-lattice and exchange-striction effects.

We conclude that for the first-order region electron-lattice and exchange-

striction effects are important, and that inclusion of these effects in an

itinerant FM model (which is in a similar spirit to the Bean-Rodbell model)

will be able to explain in some detail the magnetic and structural behavior.

We also conclude that although the itinerant model used to discuss the second-order region is rather simple, it contains in it the essential features of a more elaborate treatment.

ACKNOWLEDGMENTS

REFERENCES

*Work supported by the U. S. Atomic Energy Commission.

1. N. Menyuk, J. A. Kafalas, K. Dwight, and J. B. Goodenough, Phys. Rev. 177, 942 (1969).

2. R. H. Wilson and J. S. Kasper, Acta Cryst. 17, 95 (1964).

3. W. Köster and E. Braun, Ann. Phys. Lpz. 4, 66 (1959).

4. N. N. Sirota and E. A. Vasilev, Phys. Stat. Sol. 28, K175 (1968).

5. J. B. Goodenough, D. H. Ridgley, and W. A. Newman, in Proceedings of the International Conference on Magnetism, Nottingham, 1964 (The Institute of Physics and the Physical Society, London, 1965).

6. J. B. Goodenough and J. A. Kafalas, Phys. Rev. 157, 389 (1967).

7. J. B. Goodenough, Magnetism and the Chemical Bond (John Wiley and Sons, Inc., New York, 1963).

8. There must be 3-d itinerant states to account for the metallic like electrical conductivity.

9. E. P. Wohlfarth, J. Appl. Phys. 39, 1061 (1968); J. Phys. C [Proc. Phys. Soc.] 2, 68 (1969).

10. D. M. Edwards and E. P. Wohlfarth, Proc. Roy. Soc. (London) A 303, 127 (1968).

11. J. Mathon and E. P. Wohlfarth, Phys. Stat. Solidi 30, K131 (1968); E. P. Wohlfarth, Phys. Letters 28A, 569 (1969); E. P. Wohlfarth, Phys. Letters 31A, 525 (1970).

12. E. P. Wohlfarth and L. C. Bartel, Phys. Letters 34A, 303 (1971).

13. M. Shiga, Sol. State Comm. 7, 559 (1969).

14. The factor $\bar{I}$ in the denominator of Eq. (3) does not appear in the previous work.

15. N. D. Lang and H. Ehrenreich, Phys. Rev. 168, 605 (1968).

16. J. Hubbard, Proc. Roy. Soc. (London) A276, 238 (1963).

17. W. E. Evenson, J. R. Schrieffer, and S. Q. Wang, J. Appl. Phys. 41, 1199 (1970).

18. We shall not delve into the question of the existence of ferromagnetism within the framework of the Hubbard model, but shall assume ferro-magnetic ordering at the outset.

19. J. Kanamori, Prog. Theoret. Phys. (Kyoto) 30, 275 (1963).

20. If s-d overlap is a strong function of interatomic distance, this assumption is not valid. However, in this case the number of Mn atoms remains constant throughout the concentration range, and therefore we expect the number of magnetic d-electrons to remain more-or-less constant.

21. V. Heine, Phys. Rev. 153, 673 (1967).

22. R. C. Wayne and L. C. Bartel, Phys. Letters 28A, 196 (1968).

23. G. A. Samara and A. A. Giardini, Rev. Sci. Instr. 36, 108 (1965).

24. R. C. Wayne and L. R. Edwards, Phys. Rev. 188, 1042 (1969).

25. J. E. Schirber, Cryogenics 10, 418 (1970).

26. T. Hirone, T. Kaneko, and K. Kondo, in Physics of Solids at High Pressure, edited by C. T. Tomizuka and R. M. Emrich (Academic Press, New York, 1965), p. 298.

27. C. P. Bean and D. S. Rodbell, Phys. Rev. 126, 104 (1962).

28. R. W. Lynch, J. Chem. Phys. 47, 5180 (1967).

29. E. P. Wohlfarth, Physics and Chemistry of Solids under High Pressure, NATO Advanced Study Institute, August 1970, unpublished.

30. L. C. Bartel and E. P. Wohlfarth, Bull. Am. Phys. Soc. 16, 351 (1971).

31. If we assume a ratio I/I_b for MnSb, then I/I_b is fixed, through Eq. (6), for the solid solutions when $x > 0$. The results shown in Fig. 7 are independent of the assumed value of I/I_b for MnSb.

32. The lattice parameters for MnSb and MnAs at T = 20°C were taken from the work of B. T. M. Willis and H P. Rooksby, Proc. Phys. Soc. (London) 67B, 290 (1954). To obtain values for the intermediate solid solutions a linear extrapolation was used as the data of Ref. (3) suggest.

33. J. B. Goodenough, J. Appl. Phys. 39, 403 (1968).

34. L. C. Bartel, J. Appl. Phys. 41, 5132 (1970).

35. J. B. Goodenough, private communication.

Table I. Curie temperature T_c, $\Gamma \equiv \partial \ln T_c / \partial \ln V$, and $\overline{I}_{max}$, as calculated from Eq. (15) for $\partial \ln I_b / \partial \ln V = 0$, for various solid solutions of $MnAs_x Sb_{1-x}$ in the second-order region.

x(at.% As)	T_c	Γ	$\overline{I}_{max}$
0.00	572	2.38	1.206
0.25	458	2.97	1.180
0.50	375	3.63	1.157
0.75	292	5.18	1.122
0.80	247	6.20	1.106

FIGURE CAPTIONS

Fig. 1   Magnetic transition temperatures of $MnAs_xSb_{1-x}$ solid solutions.

       (O , ● after Sirota and Vasilev[4] and x after Goodenough et al[5].)

Fig. 2   A typical self-inductance versus temperature plot for the

       x = 0.9 solid solution.

Fig. 3   Concentration dependence of the FM to PM transition temperature

       (● present study, O after Sirota and Vasilev[4]).

Fig. 4   Concentration dependence of the initial pressure derivative of

       the FM to PM transition temperature.

Fig. 5   Temperature versus pressure magnetic phase diagram for MnAs

       and $MnAs_{0.9}Sb_{0.1}$.

Fig. 6   A comparison of $\partial T_c/\partial P$ versus T_c plots for various alloy systems.

       (O $MnAs_xSb_{1-x}$, ▲ Fe-Pt, ● Fe-Pd, and ■ Fe-Ni).

Fig. 7   A comparison of the calculated and experimental dependence of T_c

       on bandwidth (— calculated, ● experimental).
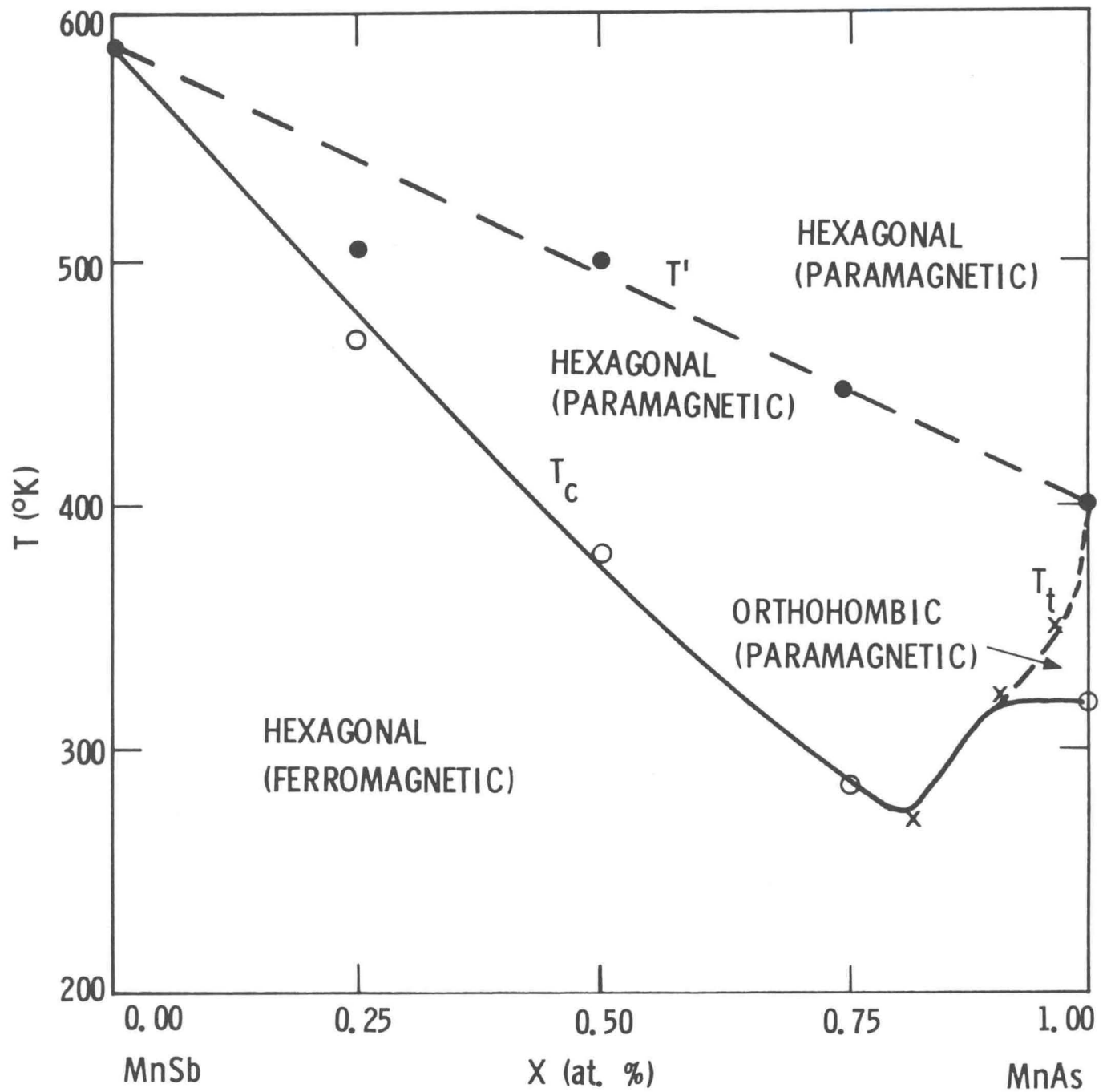
Edwards and Bartel
Fig. 1
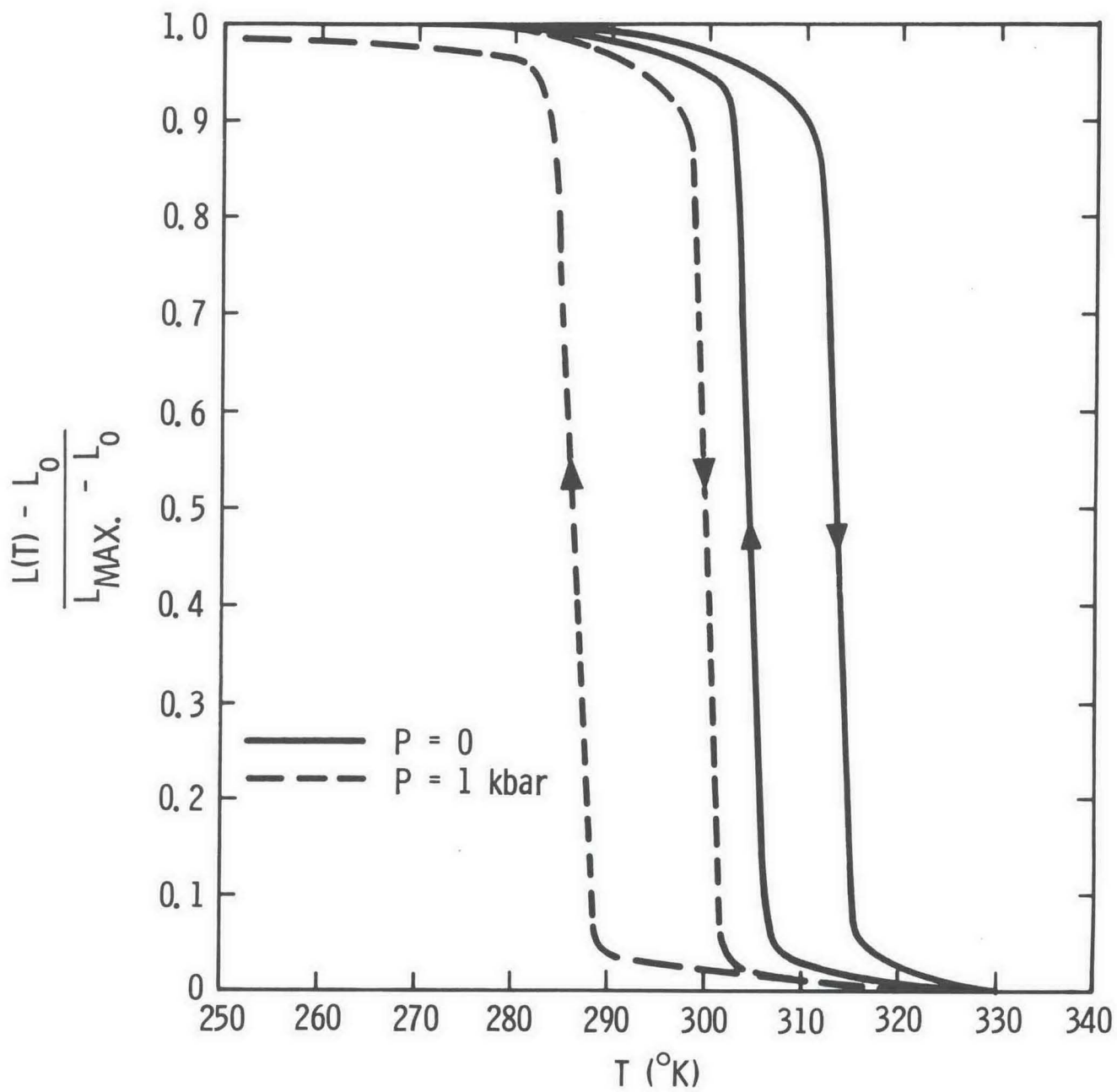
Edwards and Bartel
Fig. 2
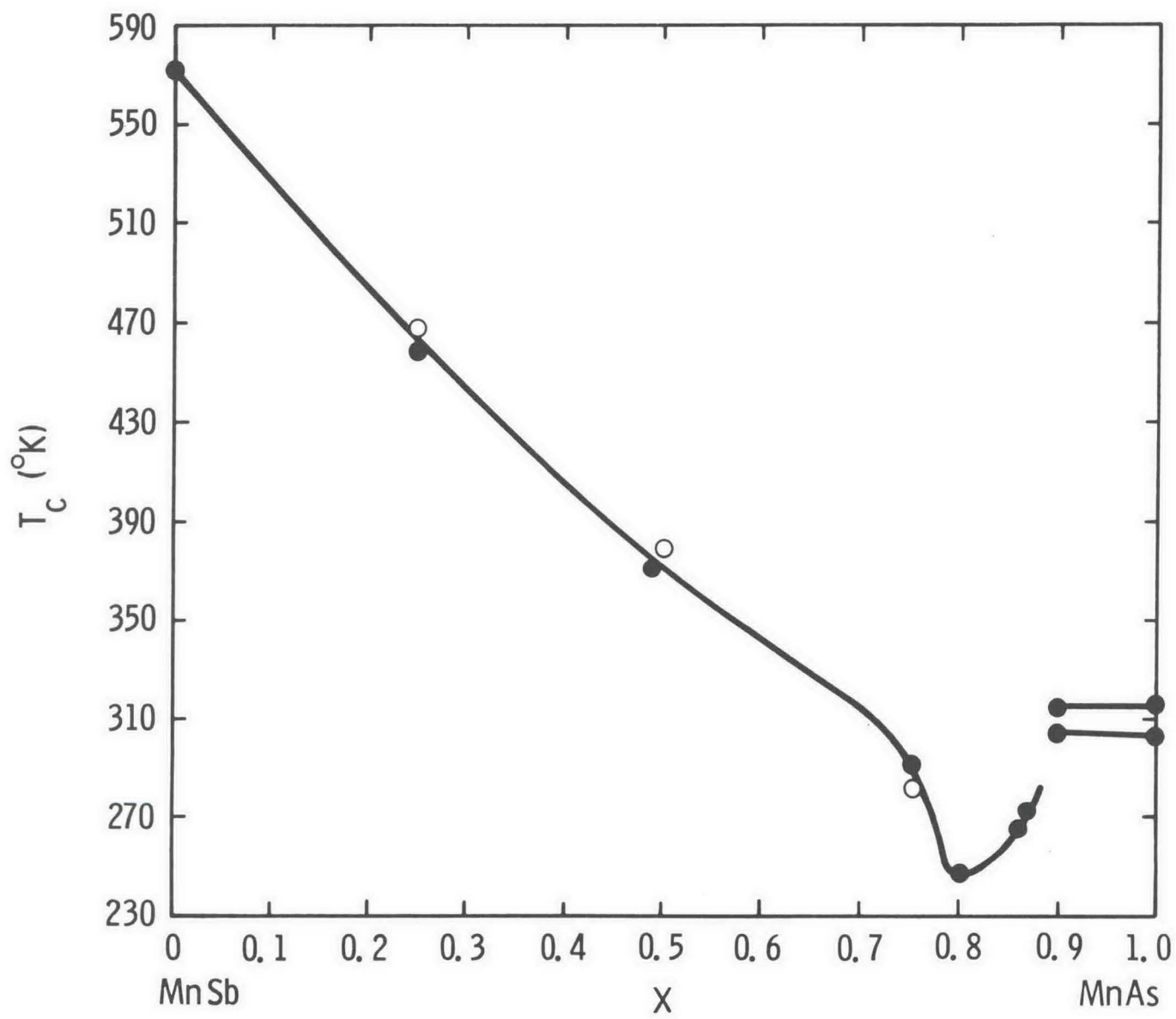
Edwards and Bartel
Fig. 3
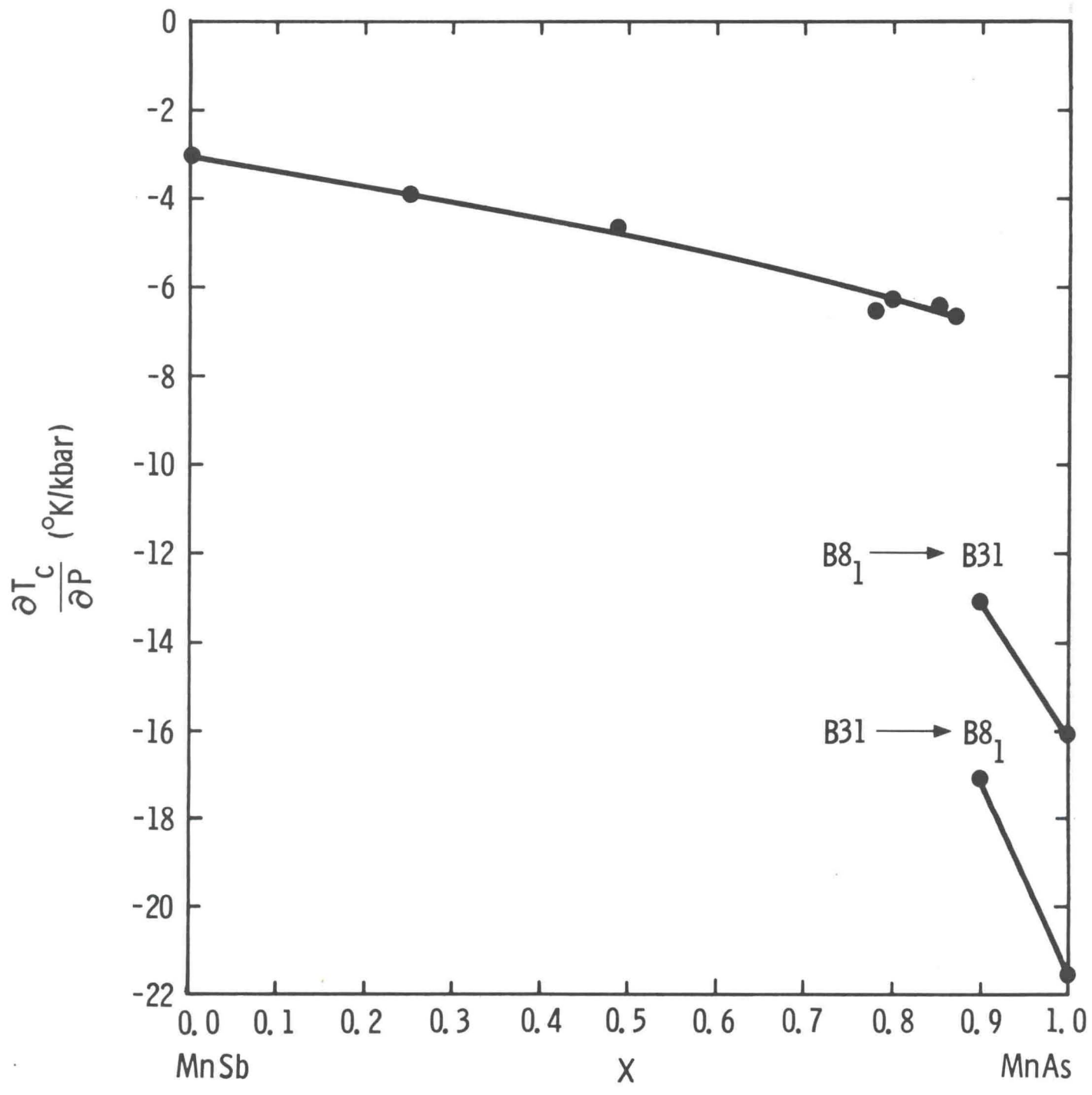
Edwards and Bartel
Fig. 4
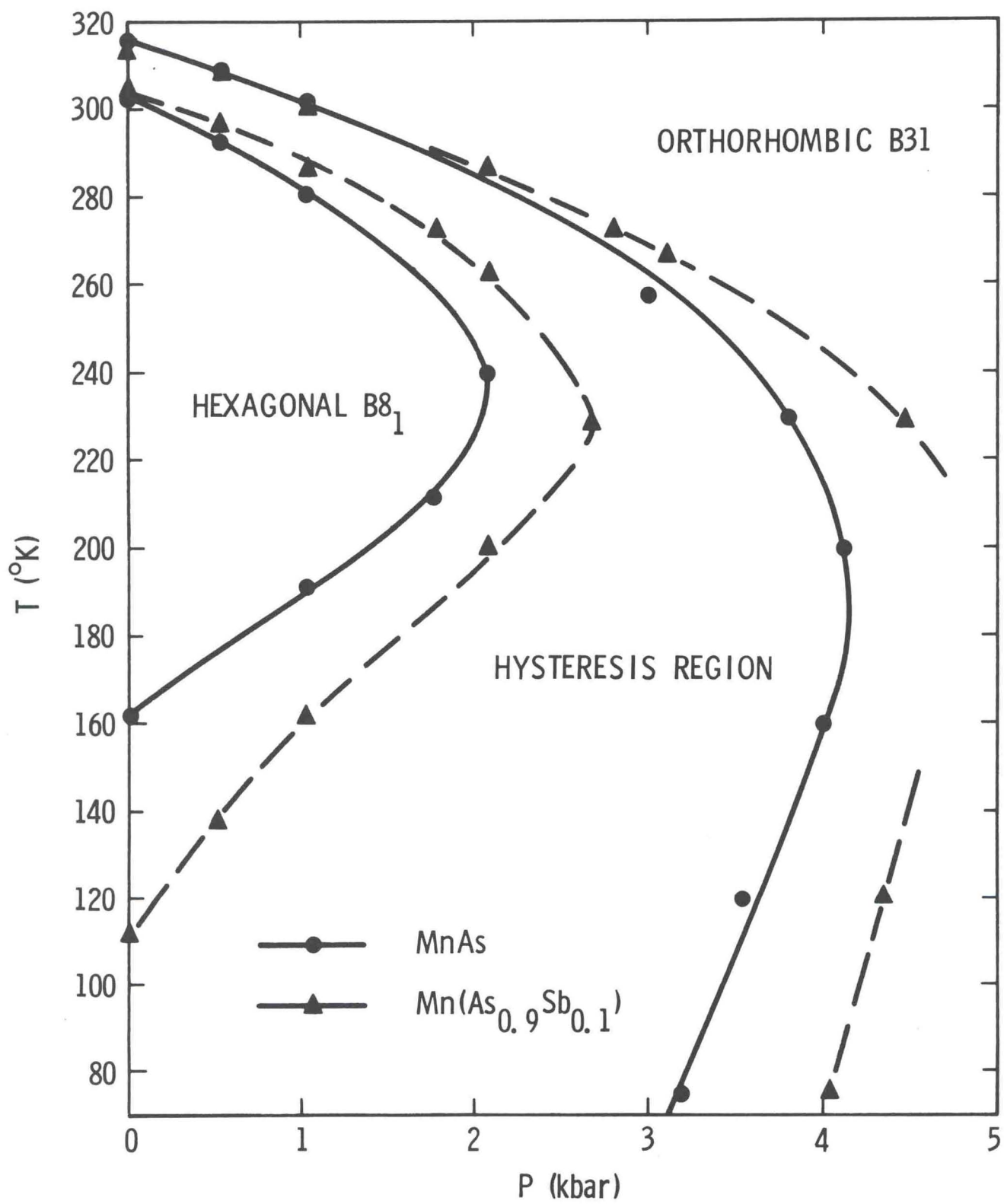
Edwards and Bartel
Fig. 5
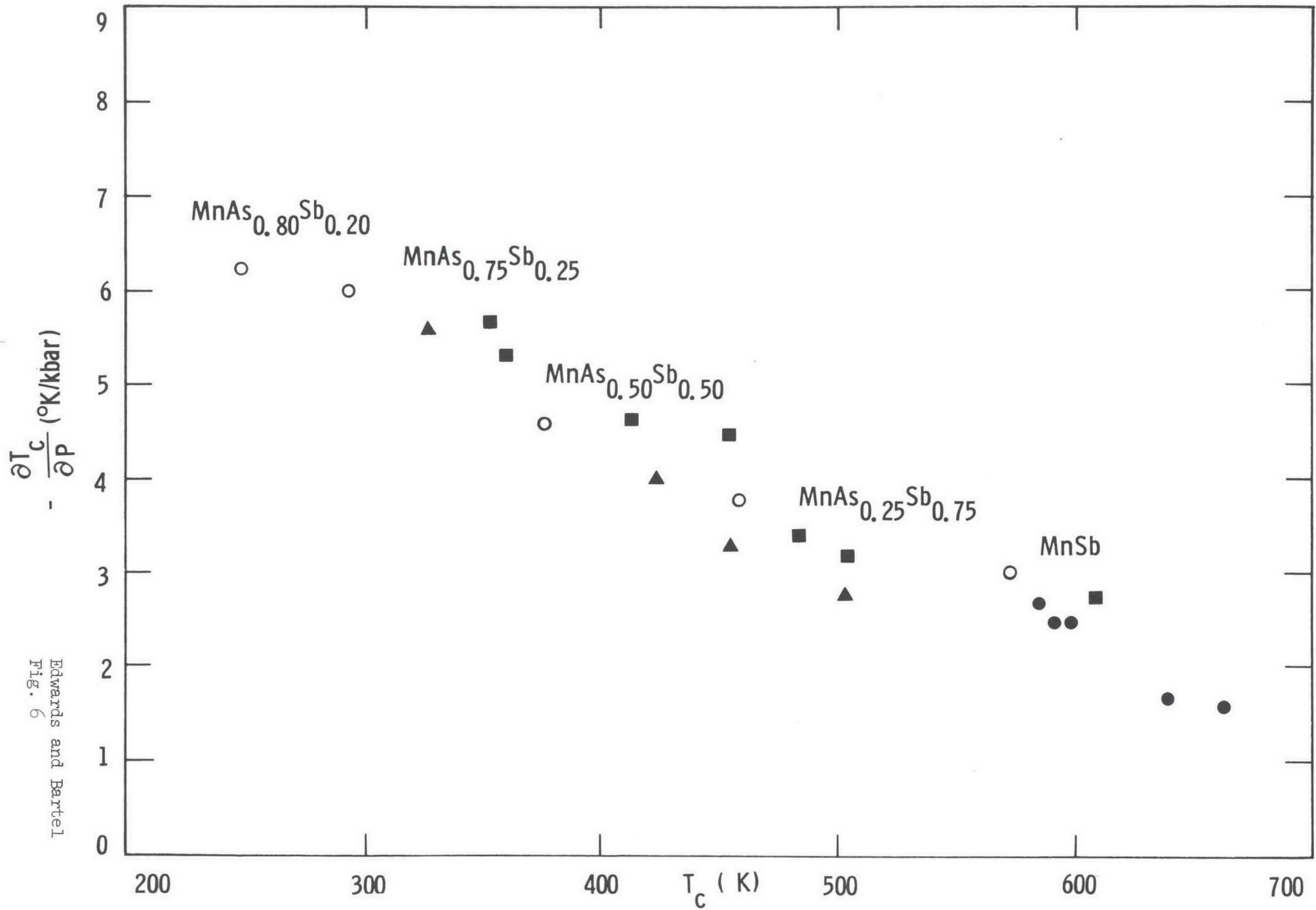
Edwards and Bartel
Fig. 6

Edwards and Bartel
Fig. 7